

Broadband absorption enhancement with ultrathin MoS_2 film in the visible regime

Jun Wu(吴俊)

Citation: Chin. Phys. B, 2021, 30 (**2**): 024208. DOI: 10.1088/1674-1056/abc3b5
Journal homepage: http://cpb.iphy.ac.cn; http://iopscience.iop.org/cpb

What follows is a list of articles you may be interested in

Geometrical condition for observing Talbot effect in plasmonics infinite metallic groove arrays

Afshari-Bavil Mehdi, Xiao-Ping Lou(娄小平), Ming-Li Dong(董明利), Chuan-Bo Li(李传波), Shuai Feng(冯帅), Parsa Saviz, Lian-Qing Zhu(祝连庆)
Chin. Phys. B, 2018, 27 (**12**): 124204. DOI: 10.1088/1674-1056/27/12/124204

Silicon nanophotonics for on-chip light manipulation

Jingshu Guo(郭敬书), Daoxin Dai(戴道锌)
Chin. Phys. B, 2018, 27 (**10**): 104208. DOI: 10.1088/1674-1056/27/10/104208

Two-dimensional materials-decorated microfiber devices for pulse generation and shaping in fiber lasers

Zhi-Chao Luo(罗智超), Meng Liu(刘萌), Ai-Ping Luo(罗爱平), Wen-Cheng Xu(徐文成)
Chin. Phys. B, 2018, 27 (**9**): 094215. DOI: 10.1088/1674-1056/27/9/094215

Absorption enhancement in thin film a-Si solar cells with double-sided SiO_2 particle layers

Chen Le, Wang Qing-Kang, Shen Xiang-Qian, Chen Wen, Huang Kun, Liu Dai-Ming
Chin. Phys. B, 2015, 24 (**10**): 104201. DOI: 10.1088/1674-1056/24/10/104201

Absorption enhancement and sensing properties of Ag diamond nanoantenna arrays

Yuan Yu-Yang, Yuan Zong-Heng, Li Xiao-Nan, Wu Jun, Zhang Wen-Tao, Ye Song
Chin. Phys. B, 2015, 24 (**7**): 074206. DOI: 10.1088/1674-1056/24/7/074206

Broadband absorption enhancement with ultrathin MoS_2 film in the visible regime*

Jun Wu(吴俊)[1,2,†]

[1] College of Electrical Engineering, Anhui Polytechnic University, Wuhu 241000, China
[2] Department of Physics, Zhejiang University of Science and Technology, Hangzhou 310023, China

(Received 13 August 2020; revised manuscript received 21 September 2020; accepted manuscript online 22 October 2020)

The broadband absorption enhancement effect in ultrathin molybdenum disulfide (MoS_2) films is investigated. It is achieved by inserting the MoS_2 film between a dielectric film and a one-dimensional silver grating backed with a silver mirror. The broadband absorption enhancement in the visible region is achieved, which exhibits large integrated absorption and short-circuit current density for solar energy under normal incidence. The optical properties of the proposed absorber are found to be superior to those of a reference planar structure, which makes the proposed structure advantageous for practical photovoltaic application. Moreover, the integrated absorption and short-circuit current density can be maintained high for a wide range of incident angles. A qualitative understanding of such broadband absorption enhancement effect is examined by illustrating the electromagnetic field distribution at some selected wavelengths. The results pave the way for developing high-performance optoelectronic devices, such as solar cells, photodetectors, and modulators.

Keywords: two-dimensional (2D) materials, transition-metal dichalcogenide, plasmonics, absorption enhancement

PACS: 42.79.Dj, 78.67.Pt, 42.25.Bs, 25.70.Ef **DOI:** 10.1088/1674-1056/abc3b5

1. Introduction

Recently, two-dimensional (2D) materials such as graphene and transition-metal dichalcogenide (TMD) have attracted tremendous research interests owing to their unique optical, electrical, and mechanical properties.[1–3] Following the success of graphene, TMD materials, such as MoS_2, WS_2, $MoSe_2$, and WSe_2, have emerged as a new class of semiconductors that exhibit distinctive properties at monolayer thickness.[4–6] One of the most appealing features of TMD materials is to enable the development of novel optoelectronic and photovoltaic devices with an atomic-scale dimension owing to their semiconducting nature and strong excitonic properties.[7–12] However, the single-pass absorption of monolayer TMD materials is usually lower than 10% within the visible wavelength.[13,14] While it is remarkably high in consideration of their single atomic thickness, it is insufficient for high performance devices when applied in the field of solar cells and photodetectors, standing as a major challenge for device development. Moreover, for photovoltaic device applications, broadband enhancement of absorption over the entire wavelength range above the band gap is highly desirable.

Under these circumstances, to realize true 2D optoelectronic and photovoltaic devices, efforts toward enhancing light–matter interactions and boosting absorption in 2D TMD materials should be made. In order to address this challenge, many configurations based on different physical mechanisms have been proposed and demonstrated. Piper *et al.* demonstrated broadband absorption enhancement in monolayer MoS_2 placed on a photonic crystal slab backed by a perfect electric conductor mirror, where an average absorption of 51% at normal incidence is achieved due to the guided mode resonances effect.[15] Bahauddin *et al.* proposed a simple plasmonic architecture, MoS_2/Ag nanoparticles/NiO_x/Al, which can achieve broadband absorption of 35% within a monolayer MoS_2.[16] Huang *et al.* proposed to combine MoS_2 film with resonant photonic structures, which enables strong absorption ($> 70\%$) in MoS_2 film (≤ 4 layers) for either narrowband incidence or broadband incidence like solar radiation.[17] Jariwala *et al.* proposed an ultrathin, near-unity, broadband absorber using TMD/metal heterostructure and applied in Schottky junction devices.[18] Long *et al.* have employed silver grating to boost the absorption in monolayer MoS_2, which is based on the excitation of multi-order magnetic polaritons.[19] Butun *et al.* demonstrated absorption enhancement in WS_2/Ag nanodisks heterostructures due to electric field localization in the vicinity of Ag nanodisks.[20] Zhang *et al.* proposed a broadband absorber made of MoS_2 film, which is polarization-insensitive, and the absorption peak maintains a high value over a large incident angle range for both polarizations.[21] Wong *et al.* reported experimental measurements for ultrathin (< 15 nm) van der Waals heterostructures, which exhibits external quantum efficiencies above 50%.[22] Kim *et*

*Project supported by the National Natural Science Foundation of China (Grant No. 61405217), the Zhejiang Provincial Natural Science Foundation, China (Grant No. LY20F050001), the Anhui Polytechnic University Research Startup Foundation, China (Grant No. 2020YQQ042), and the Pre-research Project of Natural Science Foundation of Anhui Polytechnic University, China (Grant No. Xjky2020021).

†Corresponding author. E-mail: mailswj2011@163.com

© 2021 Chinese Physical Society and IOP Publishing Ltd

al. demonstrated that the phase changes at MoS_2 interfaces enabled absorption enhancement of monolayer MoS_2 on sub-100 nm thick SiO_2/Si substrates.[23] Wang *et al.* reported a modified-MoS_2-based Tamm plasmonic structure where the perfect absorption can be achieved in the visible range.[24] Qi *et al.* demonstrated that dual-band absorption enhancement could be achieved in monolayer MoS_2 by a tapered metamaterial waveguide slab.[25] Though schemes mentioned above have demonstrated absorption enhancement in TMD materials, they still fall short of providing sufficient absorption enhancement, especially for broadband incidence like solar radiation.

In this work, the broadband light trapping effect of absorber based on MoS_2 film is investigated. First, the geometric parameters of the proposed absorber are obtained by employing the rigorous coupled-wave analysis (RCWA)[26,27] and the simulated annealing algorithm.[28,29] The absorption spectra under normal incidence are calculated and compared with those of an optimized planar reference structure with the equal thickness of MoS_2 film. Then the optical properties, including the integrated absorption, the short-circuit current density, and their angular independence, are calculated and investigated. Last, the electromagnetic field distributions at some selected wavelengths are illustrated to provide a qualitative explanation of such broadband absorption enhancement effect.

2. Design and results

A thin MoS_2 film of thickness h_m and refractive index n_m is sandwiched between a SiO_2 film and a one-dimensional silver (Ag) grating backed with an Ag mirror, as shown in Fig. 1. The grating is periodic in the x-direction and uniform in the y-direction. The grating is defined by the period d, the width $w = fd$ (where f denotes the fill factor), and the thickness h_{Ag}, the ridge material Ag, and groove material SiO_2. The thickness of the SiO_2 film is h_s. The refractive index of SiO_2 is 1.45, while the refractive indices of Ag and MoS_2in the visible regime are obtained from Refs. [30,31], respectively. The thickness of the MoS_2 film is selected as 13 nm, i.e., $h_m = 13$ nm. And the thickness of the Ag mirror is fixed to be 100 nm to prevent the transmission of light. Transverse electric (TE, with the electric field along the y axis) and transverse magnetic (TM, with the magnetic field along the y axis) polarized plane waves are incident from the air with angle θ.

To provide a figure of merit (FOM), we employed the integrated absorption, which considered absorption at all wavelengths. The integrated absorption values for TM and TE polarizations can be described by[32,33]

$$A_{TE} = \frac{\int_{300}^{800} a_{TE}(\lambda) S(\lambda)\,d\lambda}{\int_{300}^{800} S(\lambda)\,d\lambda},$$

$$A_{TM} = \frac{\int_{300}^{800} a_{TM}(\lambda) S(\lambda)\,d\lambda}{\int_{300}^{800} S(\lambda)\,d\lambda}, \quad (1)$$

where $S(\lambda)$ is the solar irradiance spectrum, which is considered as the AM1.5g solar spectral intensity distribution. $\alpha_{TE}(\lambda)$ [$\alpha_{TM}(\lambda)$] is the absorption spectra of TM (TE) polarized light calculated by RCWA, which is achieved by our home-made code (with the number of harmonics equal to 40). For the absorber in Fig. 1, the wavelength-dependent absorption spectra are calculated by employing[34]

$$\alpha(\lambda) = \frac{1}{2}\varepsilon_0 \omega\,(\mathrm{Im}\,\varepsilon(\omega)) \int_V |E|^2\,dv, \quad (2)$$

where ω is the angular frequency, ε_0 and ε denote the permittivity of vacuum and the relative permittivity of the active material, and E is the electric field. The integral is over a single period.

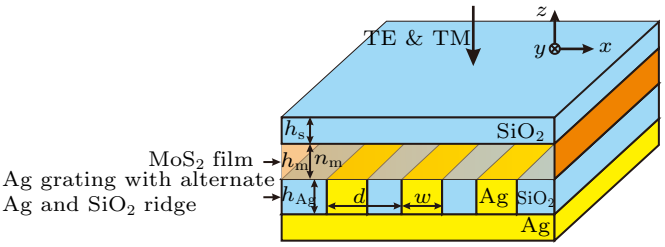


Fig. 1. Schematic diagram of the proposed MoS_2 absorber.

After numerical optimization, we obtain the geometric parameters of the proposed absorber, which is shown as follows: $d = 568$ nm, $f = 0.79$, thickness $h_{Ag} = 137$ nm, $h_s = 84$ nm. Figure 2 shows the absorption spectra of the absorber for light under normal incidence. For comparison, a reference structure, where a thin MoS_2 film with a thickness of 13 nm sandwiched between a SiO_2 film with a thickness of 72 nm and an Ag mirror, is also calculated and shown in Fig. 2. As can be seen from Fig. 2(a), the absorption of the reference planar structure is greater than 70% at wavelengths of 400–686 nm, whereas it is low in the long wavebands. The low absorption in the long wavebands is attributed to the smaller extinction coefficient of MoS_2 at wavelengths of about 700–800 nm compared to that in the short wavebands. However, when the part of the Ag mirror is patterned with the periodically grating, the absorption in MoS_2 film is enhanced strongly in the long wavebands, which leads to broadband absorption for both polarizations. Though the absorption of the reference planar structure is higher than the grating structure in the short wavebands, the overall broadband absorption performance of the grating structure is superior to that of the planar structure, which can be demonstrated by examining the integrated absorption. Under normal incidence, the average integrated absorption is 77.77% for the grating structure and 72.75% for the planar structure. Therefore, the absorber with the bottom Ag

grating structure exhibits an integrated absorption enhancement of about 7% compared to the planar structure.

Due to the intrinsic feature of metal, the Ag grating and mirror can also absorb the incident light, which is undesirable and should be minimized during the process of design. In Fig. 2(b), we show the absorption spectra in Ag grating and mirror. It is found that the absorption in Ag for TM polarization is higher than that of TE polarization in nearly the entire waveband range. In general, the average absorption in Ag is low in the short waveband and increases when the wavelength is above 700 nm.

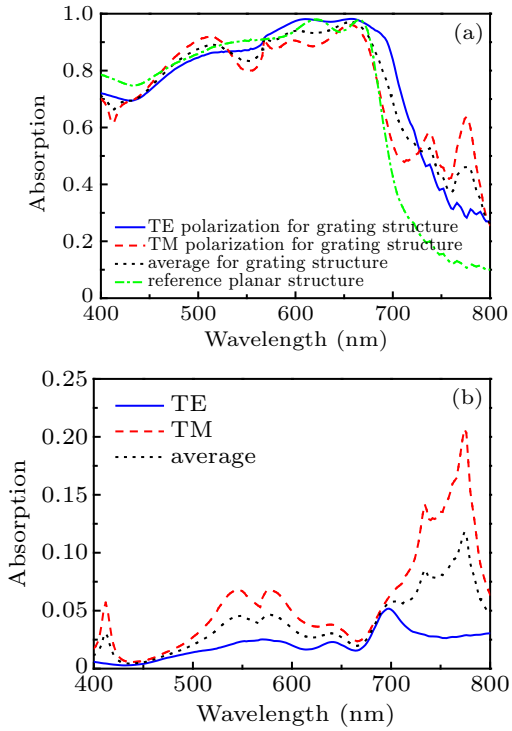


Fig. 2. The simulated absorption as a function of wavelength for light absorption in (a) MoS_2 and (b) Ag grating and Ag mirror.

3. Discussion

For the analysis above, the absorption properties are considered only for light under normal incidence. However, for practical application, the broadband absorption should be maintained over a wide range of incident angles. Under this circumstance, we calculate the absorption spectra as functions of the wavelength and incident angle for both TE and TM polarizations, which are shown in Figs. 3(a) and 3(b), respectively. For TE polarization, the absorption remains above 80% in the wavelength range of 560–666 nm with incident angle up to 60°. And the absorption is low in the long wavebands over the entire incident angle range. While for TM polarization, the absorption can remain above 80% at the incident angle of 60° in the wavelength ranges of 492–538 nm and 580–680 nm. In addition, the absorption also exhibits a decrease in the long wavebands with the increase of incident angle. The angle insensitivity in the short wavebands for both polarizations can be explained as follows. In the short wavebands, the refractive indices of MoS_2 are large, which results in an enormous refractive index contrast between the air and the MoS_2. With the increase of incident angle in air, the change of incident angle in the MoS_2 is very slow, which leads to the large angle insensitivity. In general, the broadband absorption enhancement for both polarizations can be maintained over a wide range of incident angles, which exhibits large angle insensitivity.

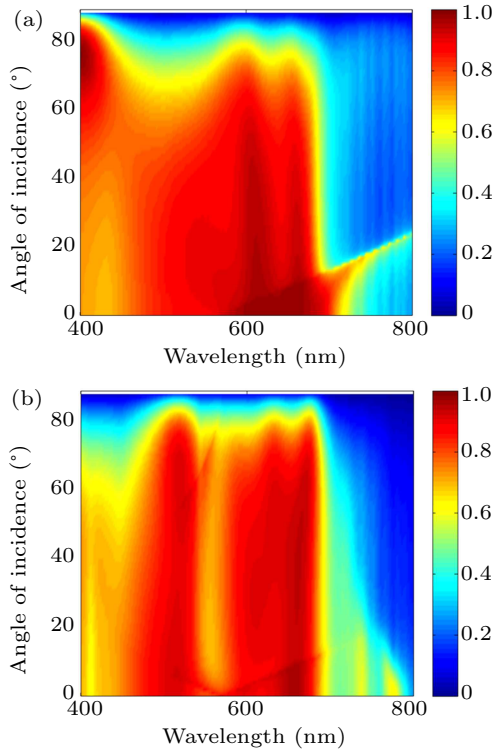


Fig. 3. Simulated absorption spectra as functions of the wavelength and angle of incidence for (a) TE and (b) TM polarization.

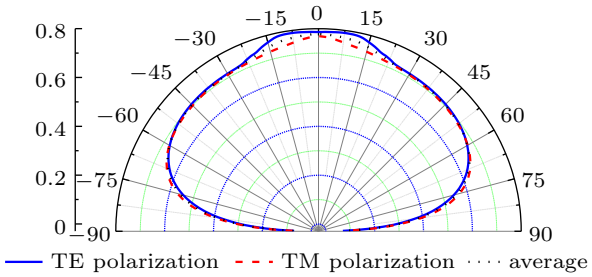


Fig. 4. Integrated absorption (TM, TE, and average) as a function of incident angle for the proposed absorber.

To intuitively confirm the angle insensitivity, we show the simulated integrated absorptions for both polarizations as a function of incident angle in Fig. 4, where the averaged integrated absorption denotes the mean of the values of TE- and TM-polarized light. For TE-polarized light, the integrated absorption remains above 60% (70%) for the incident angle up to 70° (49°), while it is higher than 60% (70%) over an angle range of 0° to 72° (0° to 43°) for TM-polarized light. In addition, the integrated absorption for TE polarization is larger

than that for TM polarization when the incident angle is less than 59°, whereas the situation is opposite when the angle is larger than 59°, indicating that the angle insensitivity of TE-polarized is better than that of TM-polarized light. In general, the averaged integrated absorption still maintains a value higher than 60% (70%) for the incident angle up to 71° (47°), indicating large angle insensitivity, which is especially attractive for real applications.

For application in the field of the solar cell, the short-circuit current density J_{sc} (mA/cm^2) is usually considered, which can be defined as follows:[35,36]

$$J_{sc} = \frac{q}{hc}\int_{\lambda_{min}}^{\lambda_{max}} \lambda\alpha(\lambda)S(\lambda)\mathrm{d}\lambda, \tag{3}$$

where the internal quantum efficiency is assumed to be 1, λ is the wavelength, q is the elementary charge, h is the Planck constant, and c is the speed of light; the integration is from $\lambda_{min} = 400$ nm to $\lambda_{max} = 800$ nm, i.e., the visible light region. To examine the potential for photovoltaic applications, we show the short-circuit current density versus the angle of incidence in Fig. 5. It is found that the short-circuit current density of TE polarization remains above 17 mA/cm^2 (15 mA/cm^2) for incident angle up to 54° (69°), whereas it still maintains a value higher than 17 mA/cm^2 (15 mA/cm^2) when the incident angle is less than 55° (72°) for TM polarization. Note that the J_{sc} value for TE-polarized light exceeds that for TM-polarized light with the incident angle in the ranges of 0–26° and 33°–51°, whereas the opposite is true for other incident angles. In general, the averaged short-circuit current density remains above 17 mA/cm^2 (15 mA/cm^2) for incident angle up to 55° (70°), which exhibits slowly decrease with increasing incident angle. Therefore, the J_{sc} value of the proposed absorber possesses large angle insensitivity, which presents a promising potential for solar energy trapping.

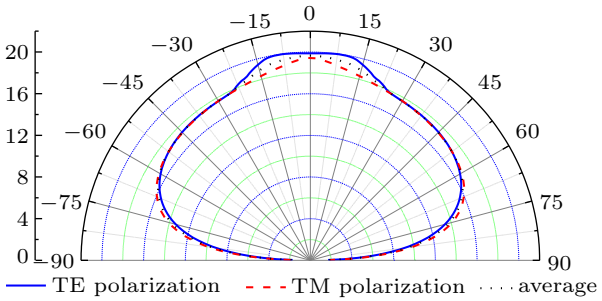


Fig. 5. Short-circuit current density J_{sc} (TM, TE, and average) as a function of incident angle for the proposed absorber. The averaged J_{sc} value is defined as the mean of the values for TE- and TM-polarized light.

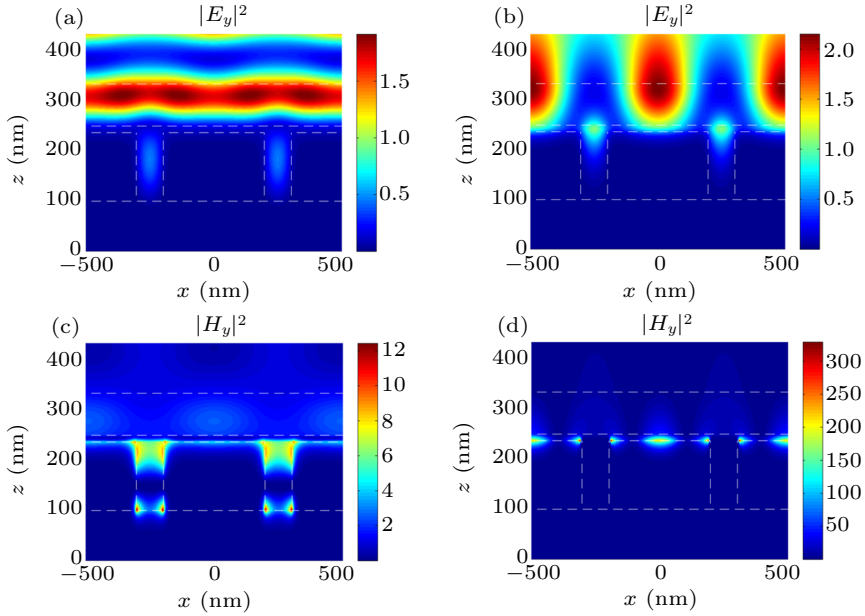


Fig. 6. Electric field distribution for TE polarization at the wavelength of (a) 400 nm and (b) 658 nm; magnetic field distribution for TM polarization at the wavelength of (c) 514 nm and (d) 776 nm. The origin of the z-axis is located at the bottom of the Ag mirror.

In order to give a qualitative understanding of such broadband absorption enhancement effect, the electromagnetic field distributions at some selected wavelengths are illustrated in Fig. 6. For TE polarization, we select the short wavelength (400 nm) and the resonant wavelength with maximum absorption (658 nm), which are shown in Figs. 6(a) and 6(b), respectively, whereas the resonant wavelengths of 514 nm (Fig. 6(c)) and 776 nm (Fig. 6(d)) are selected for TM polarization. As shown in Figs. 6(a) and 6(b), there are strongly electric field intensity enhancement and concentration in the dielectric film, MoS_2 film, and grating grooves. Moreover, the electric field intensity distributions exhibit clear standing wave profiles in the x-direction, which is a typical feature of a leaky mode. The enhanced absorption in MoS_2 film for TE polarization can be attributed to the excitation of leaky mode resonance. However, for TM polarization, the magnetic field intensity is enhanced at the interface between Ag grating and MoS_2 film and the interface between the grating ridge and grating groove at the

wavelength of 514 nm, while it is enhanced only at the interface between Ag grating and MoS_2 film at the wavelength of 776 nm. Both distributions exhibit a typical feature of surface plasmon resonance. Therefore, the enhanced absorption in MoS_2 film for TM polarization can be attributed to the excitation of plasmon resonance at the surface of Ag grating.

4. Conclusion

In summary, a broadband absorber based on ultrathin MoS_2 films is proposed and investigated. It consists of a MoS_2 film sandwiched between a dielectric film and a one-dimensional silver grating backed with a silver mirror. The broadband absorption enhancement for both polarizations in the visible region is achieved, which exhibits large integrated absorption and short-circuit current density for solar energy under normal incidence. The optical properties of the proposed absorber are found to be superior to those of a reference planar structure, which makes the proposed structure attractive for solar energy trapping application. More importantly, the integrated absorption and short-circuit current density of the proposed absorber possesses large angle insensitivity, which is particularly useful for photovoltaic applications. A qualitative understanding of such broadband absorption enhancement effect is examined by illustrating the electromagnetic field distribution at some selected wavelengths. It is believed the results will enable the development of high-performance optoelectronic devices, such as solar cells, photodetectors, and modulators.

References

[1] Bonaccorso F, Sun Z, Hasan T and Ferrari A C 2010 *Nat. Photonics* **4** 611
[2] Grigorenko A N, Polini M and Novoselov K S 2012 *Nat. Photonics* **6** 749
[3] Bao Q and Loh K P 2012 *ACS Nano* **6** 3677
[4] Xia F N, Wang H, Xiao D, Dubey M and Ramasubramaniam A 2014 *Nat. Photonics* **8** 899
[5] Wang Q H, Kalantar-Zadeh K, Kis A, Coleman J N and Strano M S 2012 *Nat. Nanotechnol.* **7** 699
[6] Xu X, Yao W, Xiao D and Heinz T F 2014 *Nat. Phys.* **10** 343
[7] Mak K F, Lee C, Hone J, Shan J and Heinz T F 2010 *Phys. Rev. Lett.* **105** 136805
[8] Splendiani A, Sun L, Zhang Y, Li T, Kim J, Chim C Y, Galli G and Wang F 2010 *Nano Lett.* **10** 1271
[9] Yu Y L, Yu Y F, Cai Y, Li W, Gurarslan A, Peelaers H, Aspens D E, Van de Walle C G, Nguyen N V, Zhang Y and Cao L 2015 *Sci. Rep.* **5** 16996
[10] Britnell L, Ribeiro R M, Eckmann A, Jalil R, Belle B D, Mishchenko A, Kim Y J, Gorbachev R V, Georgiou T, Morozov S V, Grigorenko A N, Geim A K, Casiraghi C, Castro Neto H A and Novoselov K S 2013 *Science* **340** 1311
[11] Yu Y, Yu Y, Xu C, Cai Y Q, Su L, Zhang Y, Zhang Y W, Gundogdu K and Cao L 2016 *Adv. Funct. Mater.* **26** 4733
[12] Cao L 2015 *MRS Bull.* **40** 592
[13] Bernardi M, Palummo M and Grossman J C 2013 *Nano Lett.* **13** 3664
[14] Yu Y, Hu S, Su L, Huang L, Liu Y, Jin Z, Purezky A A, Geohegan D B, Kim K W and Zhang Y 2015 *Nano Lett.* **15** 486
[15] Piper J and Fan S 2016 *ACS Photonics* **3** 571
[16] Bahauddin S, Robatjazi H and Thomann I 2016 *ACS Photonics* **3** 853
[17] Huang L, Li G, Gurarslan A, Yu Y, Kirste R, Guo W, Zhao J, Collazo R, Sitar Z, Parsons G N, Kudenov M and Cao L 2016 *ACS Nano* **10** 7493
[18] Jariwala D, Davoyan A R, Tagliabue G, Sherrott M C, Wong J and Atwater H A 2016 *Nano Lett.* **16** 5482
[19] Long L, Yang Y, Ye H and Wang L 2017 *Journal of Quantitative Spectroscopy and Radiative Transfer* **200**
[20] Butun S, Palacios E, Cain J D, Liu Z, Dravid V P and Aydin K 2017 *ACS Appl. Mater. Interfaces* **9** 15044
[21] Zhang Y, Liu W, Li Z, Cheng H, Zhang Y, Jia G, Chen S and Tian J 2017 *Appl. Phys. Lett.* **111** 111109
[22] Wong J, Jariwala D, Tagliabue G, Tat K, Davoyan A R, Sherrott M C and Atwater H A 2017 *ACS Nano* **11** 7230
[23] Kim E, Cho J W, Kim B R, Nguyen T T T, Nam Y H, Kim S K, Yoon S, Kim Y S, Lee J H and Kim D W 2018 *Adv. Mater. Interfaces* **5** 1701637
[24] Wang X Y, Wang J C, Hu Z D, Sang T and Feng Y 2018 *Appl. Phys. Express* **11** 062601
[25] Qi H L, Sang T, Yin X, Wang X and Li G Q 2020 *Appl. Phys. Express* **13** 065001
[26] Moharam M G, Grann E B, Pommet D A and Gaylord T K 1995 *J. Opt. Soc. Am. A* **12** 1068
[27] Lalanne P and Morris G M 1996 *J. Opt. Soc. Am. A* **13** 779
[28] Goffe W, Ferrier G and Rodgers J 1994 *J. Econometrics* **60** 65
[29] Shiozaki M and Shigehara M 2005 *SEI Technol. Rev.* **59** 27
[30] Johnson P B and Christy R W 1972 *Phys. Rev. B* **6** 4370
[31] Li Y, Chernikov A, Zhang X, Rigosi A, Hill H M, van der Zande A M, Chenet D A, Shih E M, Hone J and Heinz T F 2014 *Phys. Rev. B* **90** 205422
[32] Wu J 2018 *Sol. Energy* **165** 85
[33] Min C, Li J, Veronis G, Lee J Y, Fan S and Peumans P 2010 *Appl. Phys. Lett.* **96** 133302
[34] Hao J, Zhou L and Qiu M 2011 *Phys. Rev. B* **83** 165107
[35] Massiot I, Vandamme N, Bardou N, Dupuis C, Lemaître A, Guillemoles J F and Collin S 2014 *ACS Photonics* **1** 878
[36] Massa E, Giannini V, Hylton N P, Ekins-Daukes N J, Jain S, Daif O E and Maier S A 2014 *ACS Photonics* **1** 871